SciForschen
Open HUB for Scientific Research

ISSN 2381-5299

International Journal of Water and Wastewater Treatment

Research Article | Volume: 1.2 | Open Access

Adsorption Removal of Humic Acid from Micro-Polluted Water Using *in Situ* Manganese Dioxide

Yubin Zeng[1]* and Ziyang Zeng[2]

[1]*Department of Water Quality Engineering, School of Power and Mechanical Engineering, Wuhan University, Wuhan 430072, China*

[2]*Department of Chemical Engineering & Applied Chemistry, University of Toronto, Toronto, M5S 3E5, Canada*

***Corresponding author:** Yubin Zeng, Department of Water Quality Engineering, School of Power and Mechanical Engineering, Wuhan University, Wuhan 430072, China, Tel: +86 027 68772269; fax: +86 027 68772269; **E-mail:** zengyubin@whu.edu.cn

Received date: 10 Sept 2015; **Accepted date:** 30 October 2015; **Published date:** 05 November 2015.

Citation: Zeng Y, Zeng Z (2015) Adsorption Removal of Humic Acid from Micro-Polluted Water Using *in Situ* Manganese Dioxide. Int J Water and Wastewater Treatment 1(2): doi http://dx.doi.org/10.16966/2381-5299.110

Abstract

The adsorption removal of humic acid (HA) from micro-polluted water using manganese dioxide (MnO_2) formed *in situ*, which was prepared through the oxidation of $MnSO_4$ using $KMnO_4$,was investigated through batch experiments including kinetics, thermodynamics and isothermal adsorption models with online dosing mode. The results of analysis by the UV_{254} and permanganate index COD_{Mn} methods indicates that HA removal reach 29.82% and 49.99%, respectively at amount of *in situ* MnO_2 8 mg/L and contact time 2h. The kinetics data proves a closerfit to the pseudo-second order model.The isotherm data can be fit with Langmuir isotherm model well, and maximum adsorption capacity achieved 27.20 mg/g which is near to the experimental value 26.38 mg/g. Moreover, the thermodynamic analysis shows the HA adsorption on *in situ* MnO_2 is a spontaneous and exothermic process. The excellent adsorption performance and low cost of the *in situ* MnO_2 can be considered as one of the effective options to remove HA from micro-polluted water.

Keywords: *In situ* MnO_2; Humic acid; Online dosing mode; Adsorption

Introduction

Humic acid (HA) is the primary organic compound in natural water, and the molecular weight of HA is between 300 and 3000. The HA content represents 60~90% of the total organic matter in water, and it exists in the form of colloidal particles in water [1,2]. Meanwhile, HA is one of the primary potential hazards in water [3,4].

Recently, studies on using environmental materials, which widely exist in nature, as adsorbents to remove pollutants from water have drawn great attention. Among these studies, progress has been made in applying manganese dioxide (MnO_2) as environmental materials [5,6]. The natural forms of MnO_2 include δ-MnO_2, γ-MnO_2, etc, and the properties of different forms of MnO_2 are also different. Researches on using MnO_2 for removing pollutants from water have mainly focused on oxidation and adsorption. Stone reported the redox reaction between a small molecular organic compound and MnO_2 [7]. The organic compound was adsorbed on the surface of MnO_2 to form a complex, and the chemical reaction process on the surface of MnO_2 was the rate-controlling step. Liu and Tang studied the effect of mineral MnO_2 on the removal of a dye (F_3B) [8]. Their results showed that both illumination and a low pH could promote the degradation of the dye. Other researchers have also publicized the synergistic effect of MnO_2 on the oxidation and adsorption for heavy metal ions in water, such as chromium (Cr) and arsenic (As) [9,10].

On the subject of the adsorption of MnO_2, some research presented the effects of MnO_2 on the removal of uranium (VI) and thallium (I) ions under different conditions [11,12]. Bernard et al. [13] studied the primary factor that affected the adsorption of organic pollutants (e.g., HA, tannic acid, etc.) onto MnO_2 was the electronegativity of the surfaces of organic compounds. In addition, MnO_2 tended to adsorb organic pollutants with a positive surface charge. On the other hand, the resultsobtained from Liu et al. showed that δ-MnO_2 tended to adsorb HA with large molecular weights [14].

In situ MnO_2 is generated from $KMnO_4$ at the instant when $KMnO_4$ is reduced. The particles of *in situ* MnO_2 are small in size, and have a large specific surface area. Moreover, *in situ* MnO_2 is more active and has stronger adsorption ability compared with mineral MnO_2 [15,16]. Currently, studies on *in situ* MnO_2 have primarily focused on the removal of heavy metals from water, such as cadmium (Cd), strontium (Sr), and lead (Pb). However, there are few studies on using *in situ* MnO_2 to remove natural organic contaminants from micro-polluted water. Therefore, the aim of this study is to investigate the adsorption performance and behaviorof HA on *in situ* MnO_2 using the on-line adding mode. The effects of different factors on the adsorption were studied. The adsorption process is described by different kinetic and isotherm models and thermodynamics to identify the adsorption mechanism. The results give us a better understanding of the adsorption behavior of HA onto *in situ* MnO_2.

Experimental

Materials

All the reagents used were analytical grade. The concentration of stock solution $KMnO_4$ and $MnSO_4$ was 4.6 mmol/L and 6.9 mmol/L, respectively. The raw water from East Lake of Wuhan, China was used in this investigation.

Adsorption batch experiments

100 mL of raw water were added into conical flasks of 250 mL. Equivalent amounts of $MnSO_4$ solution and $KMnO_4$ solution were added

into each conical flask successively. The conical flasks were then sealed and stirred atthe speed of 200 r/min andtemperature 298K for a certain time. UV_{254} and COD_{Mn} of each filtrate (0.45 μm pore filter) were measured. The effects of adsorption time, amount of *in situ* MnO_2 and solution pH on the adsorption were studied.

The kinetics studies were investigated with sorbent dosages 8 mg/L, initial COD_{Mn} (4.31 mg/L, 13.02 mg/L) and temperatures 298K with contact time ranging from 0 to 4.0h, and samples were taken at regular intervals from the reaction solution and filtered (0.45 μm pore filter) for UV_{254} and COD_{Mn} analysis.

The adsorption isotherm experiments were studied by varying the initial HA concentration from 5.0 to 11.0 mg/L at temperatures 298K, 308K, and 318K.

All samples were prepared in duplicate, and average values of the replicated measurements were reported in all experiments. The amount of adsorbed HA, q (mg/g) was calculated using equation:

$$q = V\frac{C_0 - C_e}{M} \quad (1)$$

Where q is the amount of adsorbed HA, C_0 is the initial HA concentration, C_e is the equilibrium HA concentration, V is the volume of the solution and M is the mass of the *in situ* MnO_2.

The HA removal efficiency (%) was considered in percent as

$$\text{Removal } (\%) = 100-100\ C_e/C_0 \quad (2)$$

Analytical methods and instruments

X-ray diffraction (XRD) were performed to confirm the crystal structure and identity using X-ray Diffracto meter (Rigaku D/MAX-RB, Japan) with Cu Kα radiation in the 2θ ranges of 5°~80° at a scan rate of 1°/min. The surface structures of samples were determined using scanning electron microscopy method (SEM, JSM-5610LV, and Japan). The characterizations of the samples were carried out at their optimal working conditions.

A glass pH electrode (PHS-25, China) was used for pH measurement. The permanganate index was calculated as the chemical oxygen consumption using potassium permanganate solution as the oxidant, which is denoted as COD_{Mn}, in accordance with the standards [17]. The UV_{254} absorbance was defined as the absorbance of some organic matter in water in the presence of ultraviolet light with a wavelength of 254 nm. UV_{254} can reflect the content of natural organic matter such as HA, molecules that consists of conjugated double bonds, and aromatic compounds with C=O functional groups. The UV_{254} was measured using a UV-1600 UV/V is spectrophotometer.

Results and Discussion

XRD and SEM

The XRD pattern of the *in situ* MnO_2 is shown in Figure 1. The diffraction peak of the *in situ* MnO_2 is relatively weak and wide, which indicates low crystalline structure. Analyzing the XRD pattern as a whole, only one peak is apparent, which suggests that the purity of the *in situ* MnO_2 was relatively high. Given that the diffraction peak is at 2θ = 37.17°, a comparison with powder diffraction patterns indicates that the nature of the manganese dioxide is γ-MnO_2 [18].

Figure 2 shows the SEM image of the *in situ* MnO_2. It can be observed that the *in situ* MnO_2 particles are amorphous in nature, with a maximum diameter of approximately 120 nm. With an aging time of 30 min, the *in situ* MnO_2 is observed to coagulate into clusters. There is a tendency of increasing aggregation with increasing concentration of the *in situ* MnO_2.

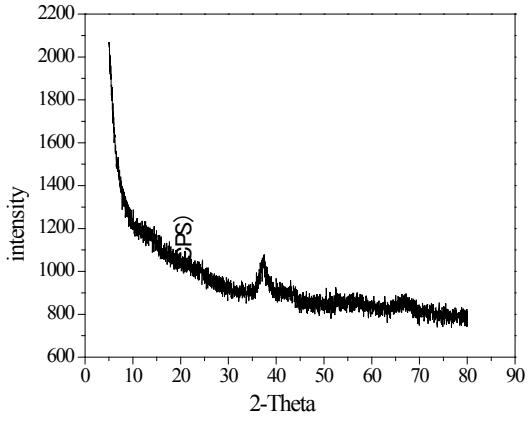

Figure 1: XRD pattern of the *in situ* MnO_2

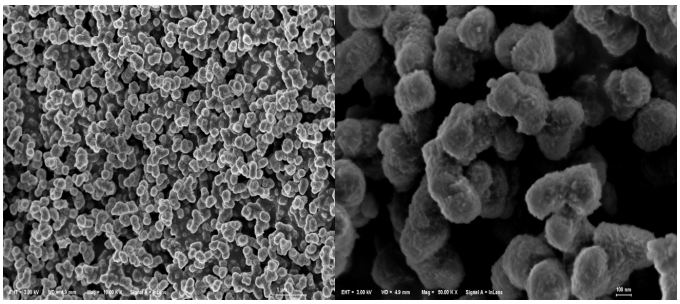

Figure 2: SEM images of the *in situ* MnO_2

Effect of adsorption time

Figure 3 displays the effect of time on adsorption of HA at a fixed initial UV_{254} 0.52 and initial COD_{Mn} 13.02 mg/L with sorbent dosages 8 mg/L at 298K. As the adsorption time increased, HA removal by UV_{254} and COD_{Mn} methods increased. When the adsorption process continued for 2h, HA removal by UV_{254} and COD_{Mn} methods were 24.00% and 44.69%, respectively. However, HA removal by COD_{Mn} method remained the same after 2 h, therefore, when the adsorption process continued for 2 h the adsorption of HA on *in situ* MnO_2 reached equilibrium.

According to adsorption theory, during the initial adsorption stage, there was no HA on the surface of and inside *in situ* MnO_2; however, the HA content in the solution was at its highest, and thus, HA could be rapidly adsorbed onto the surface of *in situ* MnO_2. As time increased, more HA was adsorbed on to *in situ* MnO_2; thus, the removal rates of HA also gradually increased. When all of the adsorption sites of *in situ* MnO_2 were saturated and in adsorption/desorption dynamic equilibrium, the adsorption capacity of *in situ* MnO_2 for HA would no longer increase as time increased, and thus, HA removal remained the same.

Effect of amount of *in situ* MnO_2

As shown in Figure 4, when more *in situ* MnO_2 was added, HA removal exhibited a clear trend, in which they first increased and then leveled off; when the amount of added *in situ* MnO_2 was 8 mg/L, HA removal by UV_{254} and COD_{Mn} methods leveled off, which were 29.82% and 49.99%, respectively.

The curve is divided into three stages. During the first stage, the added amount of *in situ* MnO_2 was 0 ~ 6 mg/L and its content was low; therefore, the generated MnO_2 could rapidly disperse into the solution.

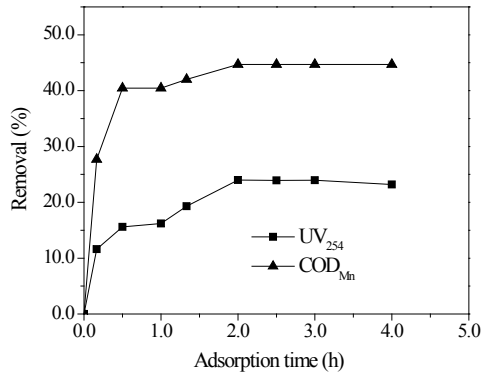

Figure 3: Effect of adsorption time (amount of *in situ* MnO_2 8 mg/L; initial UV_{254} = 0.52; initial COD_{Mn}= 13.02 mg/L; temperature 298K; pH = 8.0.)

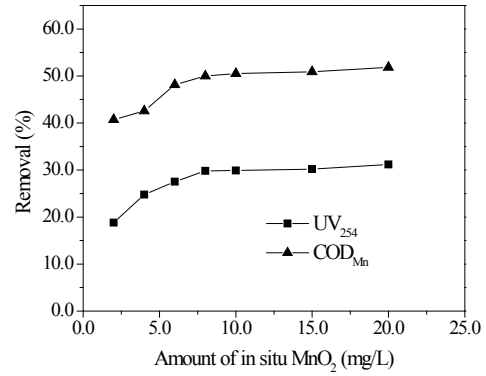

Figure 4: Effect of amount of *in situ* MnO_2 on adsorption (initial UV_{254} = 0.52; initial COD_{Mn} = 13.02 mg/L; temperature 298K; pH = 8.0; adsorption time 2h.)

In addition, the interaction between MnO_2 particles was relatively weak, and the HA content was relatively high at this time; thus, the adsorbent was "surrounded" by the adsorbate, and the adsorbent could fully adsorb the adsorbate. Consequently, as the amount of *in situ* MnO_2 increased the removal of HA by UV_{254} and COD_{Mn} methods increased linearly. During the second stage, the concentration of *in situ* MnO_2 increased from 6 mg/L to 10 mg/L. HA removal continued to increase, though at a slower rate, which might be due to the increasing concentration of *in situ* MnO_2, which would generate a certain interaction between MnO_2 particles that affects the adsorption effect. During the third stage, the content of *in situ* MnO_2 increased from 10 mg/L to 20 mg/L, whereas HA removal did not increase significantly, instead tending to level off for the reason that polymerization between MnO_2 particles could occur with the continuously increasing concentration of *in situ* MnO_2. Thus, with increasing concentration, the number of the adsorption sites of *in situ* MnO_2 did not increase, and continuously increasing the amount of adsorbent had no impact on the adsorption effect.

Effect of solution pH

As shown in Figure 5, when the pH = 2.0, HA removal by UV_{254} and COD_{Mn} methods were 49.59% and 47.52%, respectively, which were higher than those under the alkaline condition. When the pH = 4.0, HA removal decreased rapidly. However, HA removal by UV_{254} and COD_{Mn} methods increased when the pH increased to 6.0 and above 6.0.

The pH affected the adsorption of HA on *in situ* MnO_2 by two aspects: on one hand, the pH variation changes the surface properties of *in situ* MnO_2, which in turn, affects the adsorption effect. On the other hand,

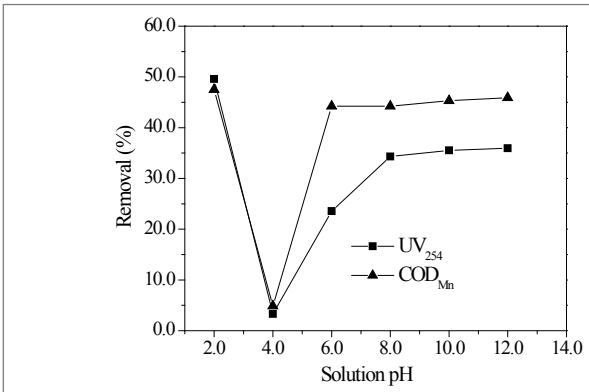

Figure 5: Effect of solution pH on adsorption (initial UV_{254} = 0.52; initial COD_{Mn} = 13.02 mg/L; amount of *in situ* MnO_2 8mg/L; temperature 298K; adsorption time 2h.)

the pH variation changes the existing forms of HA in the solution. When pH>6.0, HA existed in ionic forms (HA^- and A^{2-}) in water; *in situ* MnO_2 could adsorb HA through van der Waals forces, hydrophobic interaction, and hydrogen bond interaction. The removal of HA was approximately 40% under this condition. When pH<4.0, HA existed in the form of HA molecules in water. Because HA is difficult to dissolve in water, the interaction between *in situ* MnO_2 and HA molecules was weakened, and therefore, under this acidic condition, the adsorption effect of *in situ* MnO_2 on HA decreased. In addition, under an acidic condition, the yield of MnO_2 also decreased, which decreased the amount of the adsorbent. When the pH = 2.0, the removal of HA were higher than those under the alkaline condition, due to the fact that under the strong acidic condition (pH<3.8), *in situ* MnO_2 was a strong oxidant and thus, could oxidize HA.

Adsorption kinetics

Adsorption kinetic models can be useful to determine the mechanismof adsorption and the efficiency of the adsorbents for theremoval of pollutants. In this study, for the interpretation of the kinetic batch experimental data threedifferent kinetic models were used: (1) the pseudo-first order kinetic model (Equation 3) [19-21], (2) the pseudo-second order kinetic model (Equation 4) [20,22,23] and (3) the intraparticle diffusion model (Equation 5) [20,24].

The pseudo-first order kinetic could be shown by Equation 3:

$$\ln(q_e - q_t) = \mathrm{h}\ q_e - k_1 t \qquad 3$$

Where, q_e (mg/g) and q_t (mg/g) are the amounts of HA adsorbedon the *in situ* MnO_2 at equilibrium and at time (t), respectively. K_1 (1/h) is the pseudo-first order rate constant. K_1 and q_e were determined from the slope and intercept of the linear plot of $\ln(q_e - q_t)$ againstt, respectively. The pseudo-second order kinetic modelcan be expressed as [25]:

$$\frac{t}{q_t} = \frac{1}{k_2 q_e^{\,2}} + \frac{1}{q_e} t \qquad 4$$

$$h = k_2 q_e^{\,2} \quad \text{Equation 5}$$

Where q_e is the amount sorbed at equilibrium (mg/g), k_2 is the equilibrium rate constant of pseudo-second order (g/mg h), and h is the initial adsorption rate (mg/g h). These constants can be determined by plotting t/q_t against t.

The intraparticle diffusion kinetic (Weber-Morris diffusionmodel) is shown by the followingequation [26]:

$$q_t = k_{id} t^{1/2} + C \quad \text{Equation 6}$$

Where, K_{id} (g/mg h) is the rate constant of the in teraparticle diffusion kinetic model. The value of C and K_{id} are obtained from theintercept and slope of the linear plotted of q_t against $t^{1/2}$, respectively.

It can be seen from the Figure 6 that the adsorption capacity of *in situ* MnO_2 increased as the initial concentration of HA increased. When the initial HA concentrationincreased from 4.31 mg/L to 13.02 mg/L, the q_e of HA adsorption on *in situ* MnO_2 increased accordingly from 24.08 mg/g to 27.52 mg/g.

The adsorption of HA on *in situ* MnO_2 is classified into three stages: rapid adsorption stage, slow adsorption stage, and adsorption equilibrium stage. The rapid adsorption stage refers to the period that was within 30 min after *in situ* MnO_2 was added, where q_t reached 73.96% of the q_e. At this stage, *in situ* MnO_2 was just added into the HA solution, and there were large amounts of adsorption sites on the surface of *in situ* MnO_2. Additionally, the amount of HA in the solution was at its greatest. The second stage was the slow adsorption stage, at which time, large amounts of HA molecules had already been adsorbed onto the surface of *in situ* MnO_2, though adsorption had not reached equilibrium. *In situ* MnO_2 continued to adsorb HA in the solution; however, the adsorption rate was far slower than that during the first stage. The third stage was the adsorption equilibrium stage; when the adsorption process continued for more than 1 h (Figure 6), large amounts of HA had been adsorbed onto the surface of *in situ* MnO_2. Additionally, adsorption had essentially reached equilibrium. Therefore, the adsorption of HA on *in situ* MnO_2 was in adsorption/desorption dynamic equilibrium during this stage, and hence, the adsorption capacity would no longer increase as the adsorption time increased.

Pseudo-first order kinetics (Figure 7a) and pseudo-second order kinetics (Figure 7b) were used to fit the process of the adsorption of HA on *in situ* MnO_2. Table 1 lists the obtained related parameters. The values of R^2 from the pseudo-second order kinetics were 0.9999 and 0.9891 at different initial COD_{Mn}, and the adsorption process of HA on *in situ* MnO_2 fits more with the pseudo-second order kinetics compared with the pseudo-first order kinetics. The q_e of obtained from the pseudo-first order kinetics was 7.70 mg/g and 15.52 mg/g at different initial COD_{Mn}. However, the q_e obtained from the pseudo-second order kinetics was 24.01 mg/g and 27.20 mg/g, respectively. From the comparison with the q_e obtained from the experiment values (24.08 mg/g and 26.38 mg/g), it was more reasonable to use pseudo-second order kinetics to describe the adsorption process of HA on *in situ* MnO_2.

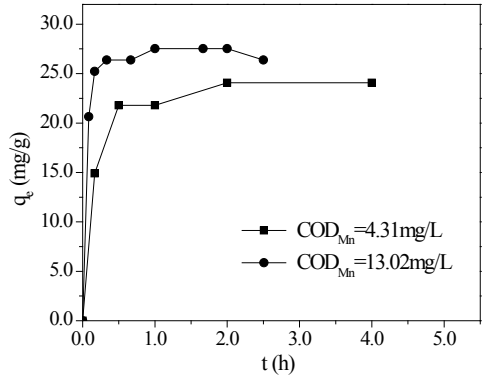

Figure 6: Adsorption capacity q_e vs. adsorption time (amount of *in situ* MnO_2 8 mg/L; initial COD_{Mn} = 4.31 mg/L, 13.02 mg/L; temperature 298K; pH = 8.0.)

An internal mass-transfer model, the Webber-Morris model, was used to further analyze this adsorption process. In the Webber-Morris pore diffusion model, if pore diffusion is a rate-controlling process, then q_t and $t^{1/2}$ should satisfy a linear relationship, where the straight line passes through the origin point [25,27]. Figure 7c shows the relationship and fitting curves of q_t and $t^{1/2}$. The values of R^2 of the adsorption process with different HAconcentrations obtained from Webber-Morris model were 0.8044 and 0.9271(Table 1). In addition, the straight line did not pass through the origin, which indicates that the internal diffusion process was notthe only rate-controlling process; butthere might be other rate-controlling processes [27].

Adsorption isotherms

Langmuir and Freundlich, isotherms models are applied in this study. Langmuir isotherm is assumed that adsorption is a monolayer adsorption and the maximum adsorption occurs when molecules adsorbed on the surface of sorbent form a saturated layer. The Langmuir equation is

$$q_e = \frac{q_m b C_e}{1 + b C_e} \text{ or } \frac{C_e}{q_e} = \frac{1}{q_m b} + \frac{C_e}{q_m} \quad (7)$$

Where q_e is the amount sorbed at equilibrium (mg/g), C_e is the equilibrium concentration (mg/L), q_m is the maximum adsorption capacity (mg/g), and b is the adsorption intensity or Langmuir coefficient related to the affinity of the binding site (L/mg).

The Freundlich isotherm can be applied to non-ideal adsorption on heterogeneous surfaces as well as multilayer adsorption and is expressed by the following equation:

$$q_e = K_F C_e^{1/n} \quad (8)$$

Where K_F and $1/n$ are the constants that are related to the adsorption capacity and the adsorption intensity, respectively. This equation can be rearranged in the linear form by taking the logarithm of both sides as

$$\ln q_e = \ln K_F + 1/n \ln C_e \quad (9)$$

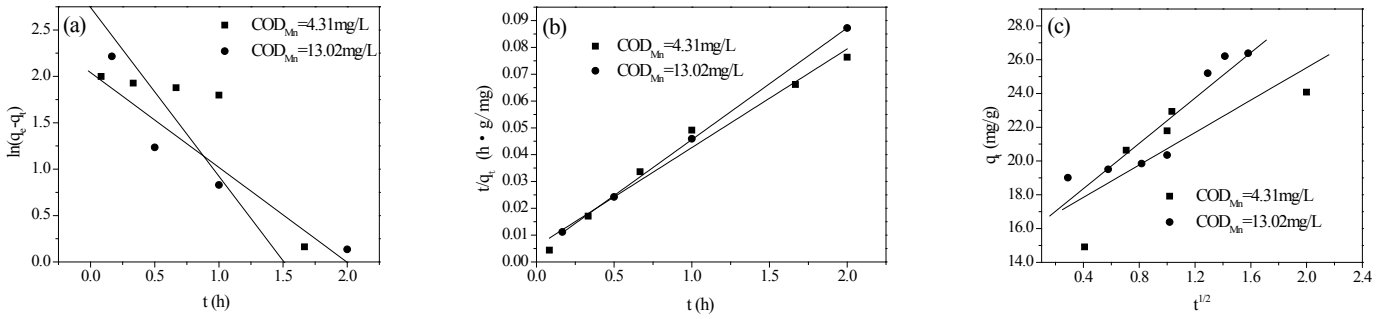

Figures 7: (a) Linearized pseudo-first-order kinetic modelcurves; (b) Linearizedpseudo-second-order kinetic modelcurves; (c) Linearized Weber-Morris diffusion model curves.

Citation: Zeng Y, Zeng Z (2015) Adsorption Removal of Humic Acid from Micro-Polluted Water Using *in Situ* Manganese Dioxide. Int J Water and Wastewater Treatment 1(2): doi http://dx.doi.org/10.16966/2381-5299.110

Initial COD_{Mn} (mg/L)	pseudo-first-order			pseudo-second-order			Weber-Morris diffusionmodel		
	q_e (mg/g)	k_1 (1/h)	R^2	q_e (mg/g)	k_2 (g/mgh)	R^2	C	k_{id} mg/gh)	R^2
4.31	7.70	1.0227	0.9404	24.01	0.2955	0.9999	15.93	4.7978	0.8044
13.02	15.52	1.8189	0.8983	27.20	0.3421	0.9891	15.68	6.7076	0.9271

Table 1: The parameters of pseudo-first-order, pseudo-second-order and Weber-Morris diffusion model kinetics

The values of K_F and $1/n$ can be calculated by plotting $\ln q_e$ against $\ln C_e$.

As shown in Figure 8, the adsorption capacity of *in situ* MnO_2 increased as the initial concentration of HA increased. When the initial concentration of HA increased to 10 mg/L, the adsorption capacity of *in situ* MnO_2 slowly leveled off.

Figures 9a and 9b represent the Langmuir and Freundlich adsorption isotherm curves of HA on *in situ* MnO_2 at temperatures 298K, 308K, and318K. Table 2 shows the parameters of the curves. The values of correlation coefficients R^2 show the adsorption behavior of HA on *in situ* MnO_2 fits more with the Langmuir model than Freundlich model, which is consistent with the conclusion obtained from the study by Zhang [28].

It can be seen from Table 2 that when using the Langmuir isothermal adsorption model, the maximum adsorption capacity of *in situ* MnO_2 for HA (q_m) decreased as the temperature increased; at 298K, q_m was as high as 161.03 mg/g; however, when the temperature reached 318K, q_m was only 36.66 mg/g because adsorption is an exothermic process, and temperature increases can cause the adsorption/desorption equilibrium to shift towards the desorption direction.

Adsorption thermodynamics

To shed light on the HA adsorption on *in situ* MnO_2, the adsorption free energy (ΔG^0), standardenthalpy (ΔH^0) and standard entropy (ΔS^0) were also calculated from the adsorption of HA on *in situ* MnO_2 at various temperatures. Based on thermodynamic theory, the basic relationship is shown as the following Equations 10 and 11, respectively:

$$\ln \frac{Q_e}{C_e} = \frac{\Delta S^0}{R} - \frac{\Delta H^0}{RT} \qquad 10$$

$$\Delta G^0 = \Delta H^0 - T\Delta S^0 \qquad 11$$

Where R is the gas constant (8.314 J mol^{-1} K^{-1}) and T is the absolute temperature (K). Thus, ΔH^0 and ΔS^0 were obtained from the slope and intercept of the line plotted by $\ln(Q_e/C_e)$ versus $1/T$, respectively.

Figure 10 show the relationship curves of $\ln q_e/c_e \sim q_e$, andthe obtained thermodynamic parameters were listed in Table 3. The free energy (ΔG^0) of the adsorption at all temperatures in the current study was negative, indicating that the adsorption process was spontaneous. The negative enthalpy change (ΔH^0) suggested that the adsorption of HA on *in situ* MnO_2 was an exothermic reaction, which was in accord with the decreasing adsorption capacity associated with increasing adsorption temperature. Also, the negative values of entropy (ΔS^0) proposed decreased randomness at the solid-solution interface during the adsorption HA onto *in situ* MnO_2 surface, and the negative entropy indicated that the mobility of HA onto the surface of *in situ* MnO_2 became more restricted as compared with that of aqueous solution. It also showed that the driving force of HA adsorption on *in situ* MnO_2 was due to an enthalpy change rather than an entropy effect.

Conclusions

In situ MnO_2 exhibits a good adsorption effect on HA in micro-polluted water. When the added amount of *in situ* MnO_2 is 8mg/L and the adsorption time is 2 h, the removal of HA by UV_{254} and COD_{Mn} methods can reach 29.36% and 49.99%, respectively. The adsorption kinetics of HA onto *in situ* MnO_2 can be well described by the pseudo-secondorder reaction model. Furthermore, the Langmuir model appears to fit the experimental data better than the Freundlich models for describing the adsorption behavior of HA from water on *in situ* MnO_2. The adsorption thermodynamics results suggest that the process of HAadsorption on

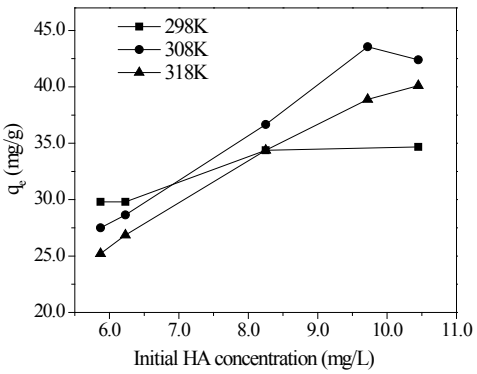

Figure 8: Adsorptioncapacities vs. initial HA concentration (pH = 8.0; adsorption time 2h; amount of *in situ* MnO_2 8mg/L.)

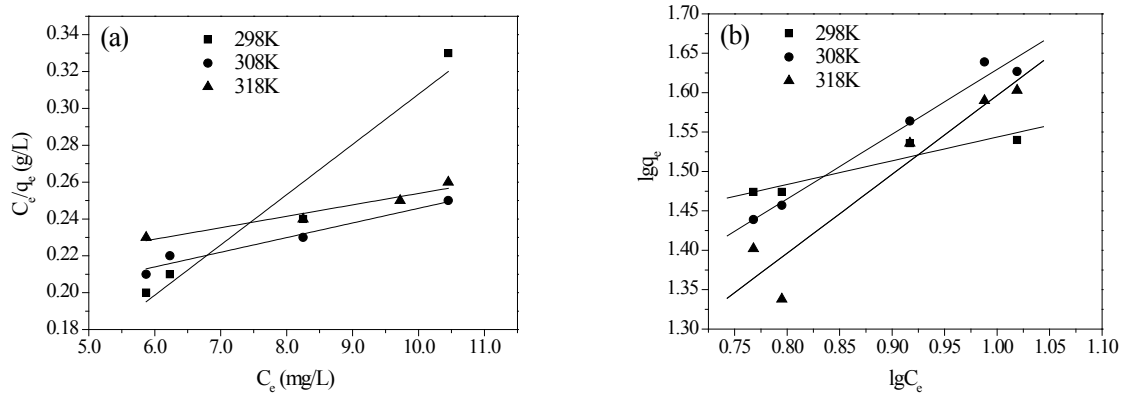

Figures 9: (a) Linearized Langmuir isotherm curves; (b) Linearized Freundlich isothermcurves

Citation: Zeng Y, Zeng Z (2015) Adsorption Removal of Humic Acid from Micro-Polluted Water Using *in Situ* Manganese Dioxide. Int J Water and Wastewater Treatment 1(2): doi http://dx.doi.org/10.16966/2381-5299.110

Temperature (K)	Langmuir			Freumdlich		
	q_m(mg/g)	b	R^2	1/n	K_F	R^2
298	161.03	0.0323	0.9477	0.3009	17.49	0.8894
308	125.79	0.0478	0.9655	0.8217	6.42	0.9791
318	36.66	0.7800	0.9440	1.0009	3.94	0.9109

Table 2: The parameters of Langmuir and Freundlich isotherms at different temperatures

Temperature (K)	K_0	ΔG^0 (kJ/mol)	ΔH^0 (kJ/mol)	ΔS^0 (J/molK)
298	3.36	-3.00	-13.57	-0.036
308	2.22	-2.04		
318	2.12	-2.02		

Table 3: Thermodynamic parameter for HA adsorption on *in situ* MnO_2

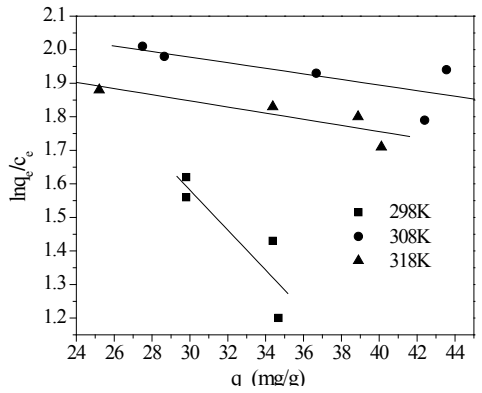

Figure 10: lnq_e/c_e~q_e relation curves

in situ MnO_2 is a spontaneous and exothermic process. Because of low cost, eco-friendly, non-toxicity and adsorption capacity of *in situ* MnO_2, this novel adsorbent canbe considered as one of the effective options to remove HA from micro-polluted water. Moreover, this study can provide scientific bases for the processes that use enhanced coagulation to remove HA from micro-polluted water.

Even so, some directions and research need to be carried out in future, these issues include: (1) influences of the nature micro-polluted water and the HA-rich surface waters for the *in situ* MnO_2, (2) evaluation of natural organic matter (NOM) removal and disinfection by-product (DBPs) control by *in situ* MnO_2, (3) feasible technological strategies using *in situ* MnO_2 to enhance the removal of NOM and to minimize DBPs formation, (4) assessment of a plant-scale application of *in situ* MnO_2 combined with coagulant to enhance coagulation on the removal of NOM.

Acknowledgment

The authors thank to the planning project on innovation and entrepreneurship training of China Universityfor the financial support.

References

1. Traversa A, D'Orazio V, Mezzapesa GN, Bonifacio E, Farrag K, et al. (2014) Chemical and spectroscopic characteristics of humic acids and dissolved organic matter along two Alfisol profiles. Chemosphere 111: 184-194.
2. Wang WD, Wang W, Fan QH, Wang YB, Qiao ZX, et al. (2014) Effects of UV radiation on humic acid coagulation characteristics in drinking water treatment processes. Chem Eng J 256: 137-143.
3. McKnight DM, Aiken GR (1998) Sources and age of aquatic humic. In: Hessen DO, Tranvik LJ (eds) Aquatic humicsubstances: Ecology and biogeochemistry. Ecological Studies 133: 9-39.
4. Xiaoli C, Yongxia H, Guixiang L, Xin Z, Youcai Z (2013) Spectroscopic studies of the effect of aerobic conditions on the chemical characteristics of humic acid in landfill leachate and its implication for the environment. Chemosphere 91: 1058-1063.
5. Li JJ, Li L, Cheng W, Wu F, Lu XF, et al. (2014) Controlled synthesis of diverse manganese oxide-based catalysts for complete oxidation of toluene and carbon monoxide. Chem Eng J 244: 59-67.
6. Luo C, Tian Z, Yang B, Zhang L, Yan SQ (2013) Manganese dioxide/iron oxide/acid oxidized multi-walled carbon nanotube magnetic nanocomposite for enhanced hexavalent chromium removal. Chem Eng J 234: 256-265.
7. Stone AT (1987) Dissolution of manganese (III/IV) oxides by substituted phenols. Environ Sci Technol 21: 979-988.
8. Liu RX, Tang HX (2000) Oxidative decolorization of direct light red F3B dye at natural surface. Water Res 34: 4029-4035.
9. Ndung'u K, Friedrich S, Gonzalez AR, Flegal AR (2010) Chromium oxidation by manganese (hydr)oxides in a California aquifer. Appl Geochem 25: 377-381.
10. Yaghi N, Hartikainen H (2013) Enhancement of Arsenite Sorption onto Oxide Coated Light Expanding Clay Aggregate by Means of Manganese Oxide. APCBEE Procedia 5: 76-81.
11. Han RP, Zou WH, Wang Y, Zhu L (2007) Removal of uranium (VI) from aqueous solutions by manganese oxide coated zeolite: discussion of adsorption isotherms and pH effect. J Environ Radioact 93: 127-143.
12. Wan SL, Ma MH, Lv L, Qian LP, Xu SY, et al. (2014) Selective capture of thallium (I) ion from aqueous solutions by amorphous hydrous manganese dioxide. Chem Eng J 239: 200-206.
13. Bernard S, Chazal P, Mazet M (1997) Removal of organic compounds by adsorption on pyrolusite (β-MnO_2). Water Res 31: 1216-1222.
14. Liu RP, Yang YL, Li GB, He WJ, Han HD (2005) Adsorptive behavior of humic acid on hydrousmanganese dioxide. Acta Scien Circu 25: 351-355.
15. Liang HF, Ma ZC, Zhang J, Hu ZJ (2005) Study on the removal of As (Ⅲ) in water by the nascent manganese dioxide. Environ Pollut Control 27: 168-170.
16. Fan CZ, Lu AH, Li Y, Wang CQ (2010) Pretreatment of actual high-strength phenolic wastewater by manganese oxide method. Chem Eng J 160: 20-26.
17. APHA–AWWA–WEF (1995) Standard Methods for the Examination of Water and Wastewater. 19th edition American Public Health Association. American Water Works Association, and Water Environment Federation. Washington DC, USA.
18. Fathy NA, El-Shafey SE, El-Shafey OI, Mohamed WS (2013) Oxidative degradation of RB19 dye by a novel γ-MnO_2/MWCNT nano composite catalyst with H_2O_2. J Environ Chem Eng 1: 858-864.
19. Shawabkeh RA, Tununji MF (2003) Experimental study and modeling of basic dye sorption by diatomaceous clay. Appl Clay Sci 24: 111-120.
20. Al-Qodah Z, Lafi WK, Al-Anber Z, Al-Shannag M, Harahsheh A (2007) Adsorption of methylene blue by acid and heat treated diatomaceous silica. Desalination 217: 212-224.
21. Daifullah AAM, Girgis BS (2003) Impact of surface characteristics of activated carbon on adsorption of BTEX. Colloid Surf A 214: 181-193.

22. Tsai WT, Hsien KJ, Chang YM, Lo CC (2005) Removal of herbicide paraquat from an aqueous solution by adsorption onto spent and treated diatomaceous earth. Bioresour Technol 96: 657-663.

23. Tsai WT, Lai CW, Su TY (2006) Adsorption of bisphenol-A from aqueous solution onto minerals and carbon adsorbents. J Hazard Mater B 134: 169-175.

24. Al-Ghouti M, Khraisheh MAM, Ahmad MNM, Allen S (2005) Thermodynamic behaviour and the effect of temperature on the removal of dyes from aqueous solution using modified diatomite: a kinetic study. J Colloid Interface Sci 287: 6-13.

25. Ho YS, McKay G (1963) Pseudo-second order model for sorption processes. Process Biochem 34: 45-465.

26. Weber WJ, Morris JC (1963) Kinetics of adsorption on carbon from solution. J Sanit Eng Div Am Soc Civ Eng 89: 31-60.

27. Shen XE, Shan XQ, Dong DM, Hua XY, Owens G (2009) Kinetics and thermodynamics of sorption of nitroaromatic compounds to as-grown and oxidized multiwalled carbon nanotubes. J Colloid Interface Sci 330: 1-8.

28. Zhang LZ, Ma J, Li X, Wang ST (2009) Enhanced removal of organics by permanganate preoxidation using tannic acid as a model compound-Role of *in situ* formed manganese dioxide. J Environ Sci 21: 872-876.